High rate molten salt cells employing barium nickel sulfide cathodes

Edward J. Plichta and Wishvender K. Behl*
US Army Electronics Technology and Devices Laboratory, LABCOM, Fort Monmouth, NJ 07703 (USA)

(Received May 29, 1991)

Abstract

Barium nickel sulfide ($BaNiS_2$) was investigated as a cathode material in high temperature molten salt cells using lithium–aluminum alloy as the anode and a eutectic mixture of lithium chloride and potassium chloride immobilized with magnesium oxide as the electrolyte. Results are presented on the cathode utilization, cathode energy and power densities obtained at current densities of 0.05 to 2.0 A/cm^2 at 400 °C. The performance of these cells is also compared with the performance of similar cells using nickel monosulfide or its mixture with barium sulfide as cathodes. The electrode reactions occurring at the positive electrode in these cells during charge and discharge operations are also discussed.

Introduction

The high temperature molten salt batteries employing lithium alloy anodes and transition metal sulfides or their mixtures (FeS, FeS_2, NiS_2, CoS_2) as cathode materials have been extensively investigated for vehicular propulsion and load-levelling applications [1]. These cells are now also being developed for high rate pulse power applications [2–5]. In the present studies, we have investigated the use of barium nickel sulfide as the cathode material in these cells for high rate applications. The results on the performance of the barium nickel sulfide cathode are presented at current densities up to 2 A/cm^2 and are also compared with the results obtained with nickel monosulfide cathodes containing 0–50 mol.% barium sulfide.

Experimental

Barium nickel sulfide ($BaNiS_2$, Cerac Pure), nickel sulfide (NiS, Cerac Pure), barium sulfide (BaS, Cerac Pure) and magnesium oxide (Maglite-D, -325 mesh powder) were used as received. The lithium–aluminum alloy powder (48 at.% lithium; Foote Mineral Company) was also used as received. The lithium chloride–potassium chloride (59:41 mol.%) eutectic electrolyte was prepared from reagent grade chemicals (Fisher Scientific Company) and purified by the usual treatment with hydrogen chloride and chlorine gases according to the procedure described previously [6]. The lithium–aluminum alloy as well as the purified eutectic electrolyte was stored in an inert atmosphere of high purity dried argon gas.

*Author to whom correspondence should be addressed.

0378-7753/92/$5.00

The cells were fabricated using 1.27 cm diameter electrode pellets. For the preparation of these pellets, the purified lithium chloride–potassium chloride eutectic electrolyte was first ground to about -325 mesh using an electric corundum mortar grinder (Brinkman Instruments Co.). The cathode pellet was made by blending 15 wt.% powdered eutectic electrolyte with 85% barium nickel sulfide or NiS and pressing at 0.12 g sample of the resulting mixture in a 1.27 cm diameter stainless steel die to a pressure of 680 kg. The separator pellet was then pressed onto the cathode pellet by pressing a 0.05 g sample of a blended mixture of 50 wt.% magnesium oxide and 50 wt.% purified lithium chloride–potassium chloride in the stainless steel die to a pressure of 680 kg. The anode pellet was similarly prepared by pressing a 0.14 g sample (65 wt.% Li–Al and 35 wt.% LiCl–KCl eutectic mixture) in a 1.27 cm diameter stainless steel die to a pressure of 1500 lbs. and the anode pellet was stacked on the other side of the separator. Each cell contained approximately three times excess lithium based upon 2 F/mole cathode capacity. Due to the hygroscopic nature of the eutectic electrolyte, the electrode pellets were pressed inside a Vacuum Atmosphere Corporation glove box containing an ultra-high purity (99.999%) argon atmosphere with a moisture content less than 10 ppm.

The cell stack was placed in a boron nitride bushing having dimensions of 1.27 cm inside diameter, 1.905 cm outside diameter and 1 cm height, which was used to guard against edge shorting. The pellet stack was held in compression through the use of a spring loaded assembly (Fig. 1) affixed with a molybdenum metal plate at the anode side and a graphite disk at the cathode side to act as current collectors. A stainless steel compression spring also helped to maintain electrical contact of the electrode pellets with the molybdenum current collector disks when the cell was heated to a working temperature of 400 °C and compensated for the slight shrinkage of the pellets due to the melting of the eutectic electrolyte. The spring loaded cell assembly was placed in a pyrex cylindrical vessel with an 'Ace-Thred' fitted with a Viton O-Ring seal top and a closed end bottom. The 'Ace-Thred' Teflon stopped used to seal the glass vessel was fitted with threaded stainless steel feedthrough connections to provide electrical connection to the positive and negative terminals of the cell. The Teflon cap was also fitted with 'Swage-lok' fittings for inserting the thermocouple and the argon gas inlet and outlet tubes.

The cell was heated overnight at 130 °C in a wire wound cylindrical furnace and a flowing atmosphere of ultra-high purity argon gas was maintained over the cell throughout the duration of the experiment. The temperature was slowly increased to

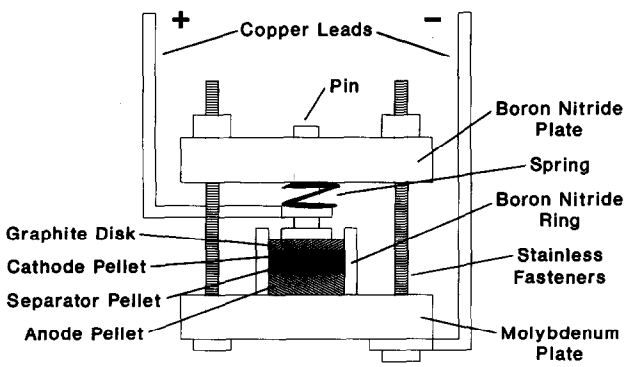

Fig. 1. Cell assembly.

400 °C over several hours and maintained at this temperature within ±2 °C using an Omega digital temperature controller (model CN5000). The temperature was measured with a chromel–alumel thermocouple using a Fluke digital thermometer (model 2176A).

The cells were galvanostatically charged and discharged using a AMEL model 545 galvanostat (Chemtech International Corporation). The galvanostat was set to the upper and lower cell voltage limits and performed the charge and discharge operations automatically within the set voltage limits at the chosen current densities. The charge–discharge curves were recorded on a Linseis model 2025 strip chart recorder and on a Nicolet digital oscilloscope (model 310). The constant current polarization curves on the cells were obtained by discharging the cells at current densities of 0.05–2 A/cm^2 and by measuring the cell potential with a Hewlett-Packard model 3456A digital voltmeter. The cells were charged at a constant current of 50 mA/cm^2 to a potential of 1.85 V.

Results and discussion

The ternary metal sulfides with the general formula, $BaMS_2$, where M is Fe, Co or Ni were first prepared by Maynard [7] who also obtained their X-ray powder patterns. The crystal structure of barium nickel sulfide and its properties have been studied by Grey and Steinfink [8]. Thus, barium nickel sulfide was found to exhibit metallic behavior with a resistivity of 1.22×10^{-2} Ω cm at 25 °C [8]. The X-ray powder diffraction pattern of barium nickel sulfide used in the present studies was confirmed by using a Phillips PW 1729 generator and Cu Kα ($\lambda = 1.540562$) radiation. The X-ray results are given in Table 1 and are in agreement with the previously reported results [8].

The thermal stability of barium nickel sulfide was checked by thermogravimetric analysis in an argon atmosphere and it was found that barium nickel sulfide is extremely stable to temperatures of about 850 °C.

The performance of barium nickel sulfide as a cathode material was studied at 400 °C using high temperature cells of the type I:

Mo|Li–Al|LiCl–KCl|$BaNiS_2$|graphite|stainless steel

Typical charge–discharge curves obtained for cycle 13 at a current density of 50 mA/cm^2 are presented in Fig. 2. The charge–discharge curves exhibited four distinct voltage plateaus. The average discharge plateau voltages for the four plateaus were found to be 1.687, 1.606, 1.375 and 1.312 V, respectively.

The discharge reactions of nickel disulfide (NiS_2) in molten lithium chloride–potassium chloride eutectic were studied by Preto *et al.* [9] using the technique of cyclic voltammetry. It was shown by these workers that nickel disulfide (NiS_2) undergoes reduction in four steps to nickel metal. The equilibrium potentials for the different discharge reactions were found to be; 1.741 V (NiS_2 to NiS), 1.586 V (NiS to Ni_7S_6), 1.552 V (Ni_7S_6 to Ni_3S_2) and 1.365 V (Ni_3S_2 to Ni).

The discharge curve obtained with cell I (Fig. 2) exhibited a voltage plateau at about 1.687 V. The average plateau voltage is higher than the equilibrium potentials reported by Preto *et al.* [9] for the reduction of nickel monosulfide (NiS) to lower nickel sulfides. The higher plateau voltage suggests the presence of some nickel disulfide (NiS_2) in barium nickel sulfide. Thus, the average plateau voltage is comparable to the equilibrium potential of 1.741 V reported by Preto *et al.* [9] for the reduction of NiS_2 to NiS. The presence of nickel disulfide in barium nickel sulfide may be explained

TABLE 1

X-ray powder diffraction results for $BaNiS_2$ (Cu Kα = 1.540562 Å)

(*hkl*)	$2\theta_{hkl}$	d_{hkl}	Relative intensities I/I_1(obs.)
100	20.10	4.414	15
101	22.58	3.935	29
110	28.55	3.124	100
111	30.40	2.938	40
112	35.08	2.556	45
103	36.51	2.459	49
200	40.82	2.209	60
201	42.05	2.147	34
210	45.80	1.980	23
211	47.04	1.930	28
212	50.50	1.806	38
203	51.50	1.773	55
213	55.85	1.645	45
220	59.00	1.564	40
221	59.90	1.543	53
300	62.80	1.478	25
301	63.85	1.457	22
310	66.70	1.401	45
311	67.06	1.394	48
312	70.50	1.335	35
303	71.40	1.320	25
313	75.00	1.265	30
320	77.60	1.229	12
321	78.50	1.217	16
322	81.15	1.184	22
323	85.50	1.135	17
400	88.80	1.101	33
401	89.00	1.099	26
410	91.60	1.074	15
330	95.00	1.045	25
331	95.90	1.037	18
332	98.60	1.016	16

by the non-stoichiometry of the synthesized barium nickel sulfide. Thus, it has been reported [8] that the synthesized barium nickel is represented by the formula, $BaNiS_{2+x}$, where $x = 0$–0.4 Therefore, the first voltage plateau in the discharge curve (Fig. 1) may be attributed to the reduction of $BaNiS_{2+x}$ to $BaNiS_2$ according to the equation:

$$BaNiS_{2+x} + 2x\text{Li–Al} \rightleftharpoons BaNiS_2 + xLi_2S + 2x\text{Al} \quad (1)$$

Since only a small amount of excess sulfur ($x = 0$–0.4) is present in barium nickel sulfide, the voltage plateau corresponding to reaction (1) is rather small.

Since the equilibrium potentials for the reduction of NiS to Ni_7S_6 (1.586 V) and the subsequent reduction of the latter to Ni_3S_2 (1.552 V) are separated by only 34 mV, the discharge curves did not exhibit separate plateaus for these reactions at high current densities. Thus the second voltage plateau in the discharge curves at high discharge rates (Fig. 3) may be ascribed to the reaction:

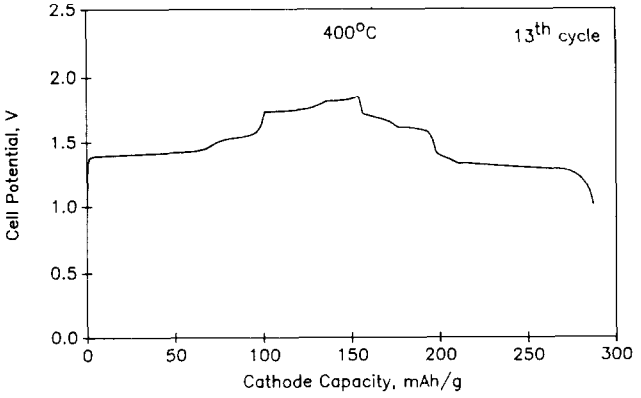

Fig. 2. Typical charge–discharge cycle of the cell LiAl/LiCl–KCl/$BaNiS_2$ at 400 °C.

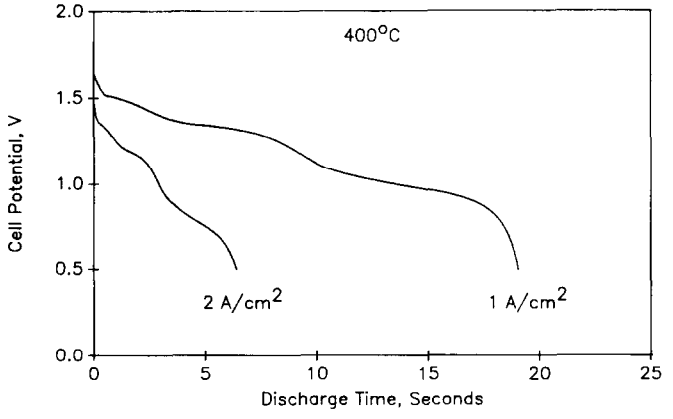

Fig. 3. Typical discharge curves of the cell LiAl/LiCl–KCl/$BaNiS_2$ at current densities of 1 and 2 A/cm^2 at 400 °C.

$$3BaNiS_2 + 2Li\text{–}Al \rightleftharpoons Ni_3S_2 + 3BaS + Li_2S + 2Al \quad (2)$$

The fourth voltage plateau in the discharge curve (Fig. 2) with an average plateau voltage of 1.312 V may be attributed to the reduction of Ni_3S_2 to nickel metal according to the reaction:

$$Ni_3S_2 + 4Li\text{–}Al \rightleftharpoons 3Ni + 2Li_2S + 4Al \quad (3)$$

The average plateau voltage is comparable to the equilibrium potential of 1.365 V reported for this reaction [9].

Cell I was also discharged at other current densities in the range of 0.05 to 2 A/cm^2 and typical discharge curve obtained at very high discharge rates of 1 and 2 A/cm^2 are presented in Fig. 3. Unlike the discharge curve obtained at the lower discharge rate (Fig. 2), the discharge curves at 1 and 2 A/cm^2 exhibited only three voltage plateaus. Similar discharge curves were obtained at other discharge rates and the energy densities, power densities and cathode utilizations based on barium nickel sulfide at different discharge rates are summarized in Table 2.

TABLE 2

Cathode utilization, cathode energy and power densitites in LiAl/LiCl–KCl/X cells where X is $BaNiS_2$, NiS or NiS–BaS mixture

Cathode	Discharge current density (A/cm)	Discharge voltage limit (V)	Average cell voltage (V)	Cathode utilization[a] (%)	Cathode energy density[b] (kJ/kg)	Cathode power density[b] (kW/kg)
$BaNiS_2$	0.05	1.0	1.470	65	705	0.9
	0.1	1.0	1.448	57	613	1.8
	0.2	1.0	1.380	56	570	3.4
	0.5	1.0	1.336	39	391	8.3
	1.0	0.5	1.158	32	275	14.4
	2.0	0.5	0.934	22	150	23.3
NiS	0.05	1.0	1.338	34	958	1.0
	0.1	1.0	1.304	25	701	2.0
	0.2	1.0	1.270	16	436	3.8
	0.5	1.0	1.228	7	192	9.2
	1.0	0.5	1.062	4	93	15.9
	2.0	0.5	0.950	4	88	28.4
75 mol.% NiS	0.05	1.0	1.373	56	1005	1.0
25 mol.% BaS	0.1	1.0	1.370	47	839	2.1
	0.2	1.0	1.277	32	534	3.8
	0.5	1.0	1.261	10	172	9.4
	1.0	0.5	0.980	15	192	14.6
	2.0	0.5	0.791	10	98	23.6
50 mol.% NiS	0.05	1.0	1.340	56	551	1.0
50 mol.% BaS	0.1	1.0	1.270	46	429	1.9
	0.2	1.0	1.240	33	300	3.7
	0.5	1.0	1.180	16	141	8.8
	1.0	0.5	0.911	11	75	13.6
	2.0	0.5	0.740	8	42	22.1

[a]Cathode utilization based only on active cathode component assuming a theoretical capacity of 2 F/mole.

[b]Energy and power densities based on cathode weight excluding electrolyte. Cathodes contained 15 wt.% electrolyte.

From the data presented in Table 2, it can be seen that cell I is capable of delivering high energy densities and high power densities needed for pulse power applications. Further, the cell also showed good cycle life and was capable of being charged and discharged for over one hundred cycles.

Cell I was also investigated using nickel sulfide (NiS) as the cathode. The discharge curves obtained with this cell exhibited only two voltage plateaus corresponding to the reduction of NiS to Ni_3S_2 followed by the reduction of the latter to nickel metal and lithium sulfide. Since nickel sulfide (NiS) did not contain any nickel disulfide (NiS_2), the discharge curves did not exhibit any higher voltage plateau as was observed when barium nickel sulfide was used as the cathode material. A typical discharge curve at a current density of 1 A/cm^2 obtained with cell I using nickel sulfide (NiS) as the cathode material is presented in Fig. 4 along with the discharge curve for cell I with barium nickel sulfide ($BaNiS_2$) as the cathode material. It can be seen that

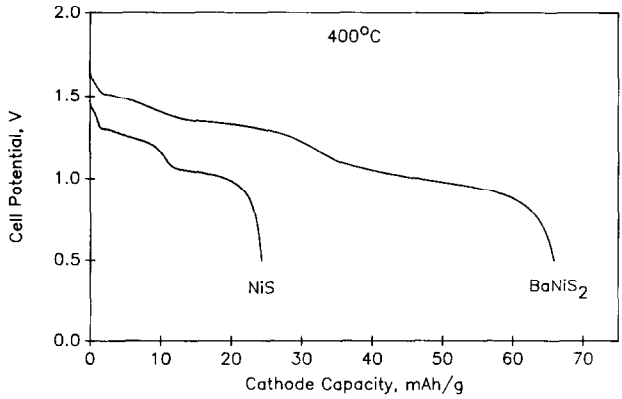

Fig. 4. Typical discharge curves of the cell LiAl/LiCl–KCl/X, where X is $BaNiS_2$ or NiS, at a current density of 1 A/cm^2 at 400 °C.

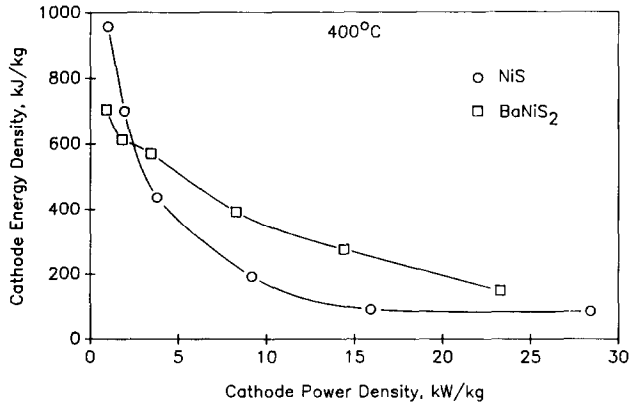

Fig. 5. Cathode energy densities vs. cathode power densities obtained in cells LiAl/LiCl–KCl/X, where X is $BaNiS_2$ or NiS, at 400 °C.

at a current density of 1 A/cm^2, the cathode capacities obtained with barium nickel sulfide were about 2.5 times higher than those obtained with nickel sulfide. The performance of the two cathode materials is compared in Fig. 5 which presents plots of the cathode energy densities versus the cathode power densities. It was found that cells with barium nickel sulfide as the cathode material delivered higher energy densities at high discharge rates than the cells using nickel monosulfide as the cathode material. This suggested that the performance of cell I with nickel monosulfide as the cathode material can perhaps be improved by incorporation of barium sulfide in the cathode structure. Thus, a number of cells were investigated where the cathode material consisted of mixtures of nickel monosulfide and barium sulfide.

The discharge curves obtained at a current density of 1 A/cm^2 with cell I using mixtures of nickel sulfide and barium sulfide (0, 25 and 50 mol.% BaS) are presented in Fig. 6 and the cathode utilization, cathode energy density and power density data are summarized in Table 2. The cathode energy densities obtained in cell I with mixtures of nickel sulfide and barium sulfide as cathode materials at various discharge

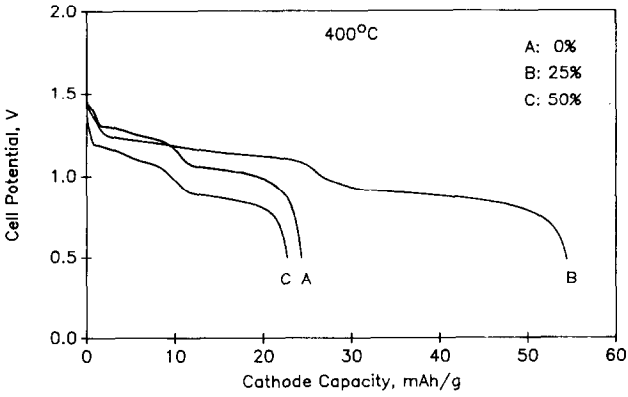

Fig. 6. Typical discharge curves of the cell LiAl/LiCl–KCl/NiS-BaS (0–50 mol.% BaS) at a current density of 1 A/cm^2 at 400 °C.

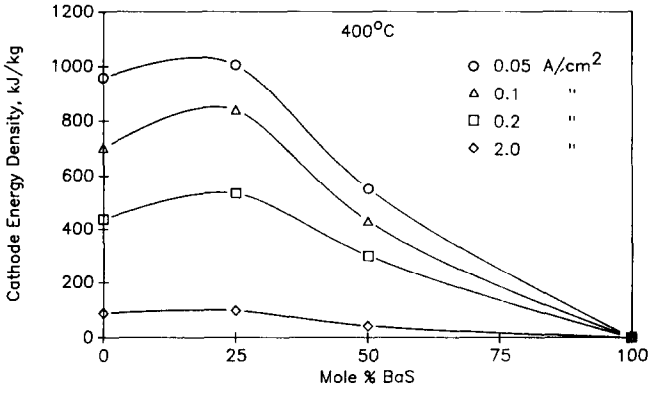

Fig. 7. Cathode energy densities obtained for the cell LiAl/LiCl–KCl/NiS–BaS(0–50 mol.% BaS) at current densities of 0.05 to 2.0 A/cm^2 at 400 °C.

rates are also plotted in Fig. 7 as a function of barium sulfide mole fraction. It was found that the addition of 25 mol.% barium sulfide to nickel sulfide resulted in an increase in the cathode utilization as well as an increase in the cathode energy density. On the other hand, addition of 50 mol.% barium sulfide was deleterious and resulted in lower cathode utilization and lower cathode capacities. Even though the incorporation of 25 mol.% barium sulfide with nickel sulfide in the cathode structure resulted in higher cathode energy densities than those obtained with nickel sulfide alone, the cathode capacities were less than those obtained with barium nickel sulfide cathodes (see Table 2). The higher capacities obtained with barium nickel sulfide cathodes at high discharge rates may be attributed to higher cathode utilization due to the low resistivity [8] of barium nickel sulfide cathodes. Further improvements in cathode energy densities may be achieved by substituting a lighter alkaline earth cation such as magnesium, calcium or strontium for barium in the ternary barium nickel sulfide.

Conclusions

The high temperature molten salt cells were investigated employing lithium–aluminum alloy as the anode, a eutectic mixture of lithium chloride and potassium chloride as the electrolyte and barium nickel sulfide as the cathode at 400 °C. It was found that the use of $BaNiS_2$ cathodes in these cells resulted in higher cathode utilization and energy densities at high discharge rates than those obtained with cathodes based on nickel monosulfide or its mixtures with barium sulfide. It was further found that these cells are capable of delivering high energy densities and power densities at current densities in excess of 1 A/cm^2 required for pulse power applications.

References

1 J. R. Selman, in R. P. Tischer (ed.), *The Sulfur Electrode*, Academic Press, New York, 1983, Ch. VI, pp. 219–234.
2 L. Redey, *22nd IECEC*, American Institute of Aeronautics and Astronautics, Washington, DC, 1987, p. 1091.
3 H. F. Gibbard, *J. Power Sources, 26* (1989) 81.
4 H. N. Sieger, *Proc. 34th Int. Power Sources Symp.*, Institute of Electrical and Electronics Engineers, Inc., New York, 1990, p. 334.
5 N. Papadakis, *Proc. 34th Int. Power Sources Symp.*, Institute of Electrical and Electronics Engineers, Inc., New York, 1990, p. 339.
6 W. K. Behl, *J. Electrochem. Soc., 118* (1971) 889.
7 J. T. Maynard, *US Patent No. 2 770 528* (Nov. 13, 1956).
8 I. E. Grey and H. Steinfink, *J. Am. Chem. Soc., 92* (1970) 5093.
9 S. K. Preto, Z. Tomczuk, S. von Winbush and M. F. Roche, *J. Electrochem. Soc., 130* (1983) 264.